PASJ: Publ. Astron. Soc. Japan **59**, S785–S791, 2007 November 30

Evolution of the Sheared Magnetic Fields of Two X-Class Flares Observed by Hinode/XRT*

Yingna SU,[1,2,3] Leon GOLUB,[1] Adriaan VAN BALLEGOOIJEN,[1] Edward E. DELUCA,[1] Kathy K. REEVES,[1]
Taro SAKAO,[4] Ryouhei KANO,[5] Noriyuki NARUKAGE,[4] and Kiyoto SHIBASAKI[6]
[1]*Harvard-Smithsonian Center for Astrophysics, 60 Garden Street, Cambridge, MA 02138, USA*
ynsu@head.cfa.harvard.edu
[2]*Purple Mountian Observatory, 2 West Beijing Road, Nanjing 210008, P.R.China*
[3]*Graduate University of Chinese Academy of Sciences 19A Yuquanlu, Beijing 100049, P.R.China*
[4]*Institute of Space and Astronautical Science, Japan Aerospace Exploration Agency, 3-1-1 Yoshinodai, Sagamihara, Kanagawa 229-8510*
[5]*National Astronomical Observatory of Japan, 2-21-1 Osawa, Mitaka, Tokyo 181-8588*
[6] *Nobeyama Solar Radio Observatory, NAOJ, Minamimaki, Minamisaku, Nagano 384-1305*

(Received 2007 May 31; accepted 2007 August 17)

Abstract

We present multi-wavelength observations of the evolution of the sheared magnetic fields in NOAA Active Region 10930, where two X-class flares occurred on 2006 December 13 and December 14, respectively. Observations made with the X-ray Telescope (XRT) and the Solar Optical Telescope (SOT) aboard Hinode suggest that the gradual formation of the sheared magnetic fields in this active region is caused by the rotation and west-to-east motion of an emerging sunspot. In the pre-flare phase of the two flares, XRT shows several highly sheared X-ray loops in the core field region, corresponding to a filament seen in the TRACE EUV observations. XRT observations also show that part of the sheared core field erupted, and another part of the sheared core field stayed behind during the flares, which may explain why a large part of the filament is still seen by TRACE after the flare. About 2–3 hours after the peak of each flare, the core field becomes visible in XRT again, and shows a highly sheared inner and less-sheared outer structure. We also find that the post-flare core field is clearly less sheared than the pre-flare core field, which is consistent with the idea that the energy released during the flares is stored in the highly sheared fields prior to the flare.

Key words: Sun: corona — Sun: filaments — Sun: flares — Sun: magnetic fields — Sun: X-rays, gamma rays

1. Introduction

Solar flares, prominence eruptions, and coronal mass ejections (CMEs) are magnetic phenomena thought to be powered by the magnetic free energy (i.e., the difference between the total magnetic energy and the potential field magnetic energy) stored in the corona prior to eruption. The storage of free energy requires a nonpotential magnetic field, and is therefore associated with a shear or twist in the coronal field away from the potential, current-free state (Priest & Forbes 2002). One indication of such a stressed magnetic field is the presence of a prominence. Another important indicator of a stressed magnetic field is the presence of sigmoid signatures, discovered by Rust and Kumar (1997) and Canfield et al. (1999) with Yohkoh/SXT. Indeed, they have found that sigmoidal active regions to be the most likely to erupt.

A strong-to-weak shear motion of the hard X-ray footpoints during the flare was firstly reported by Masuda et al. (2001). This motion was claimed to be a common feature in two-ribbon flares by Su et al. (2007a), who identified this motion in 86% of 50 two-ribbon flares observed by TRACE. A further detailed study by Su et al. (2007b) shows that the change of the shear angle of the footpoints during the flare is positively correlated with the intensity of solar flare/CME events for an 18-event sample. Studies of both shear motion and contracting motion of the footpoints in several individual flares were carried out by Ji et al. (2006, 2007). A detailed interpretation of this shear motion was given by Su et al. (2006), based on a three-dimensional model for eruptive flares (Moore et al. 2001, and references therein). According to this model, the pre-flare configuration contains a highly sheared core field inside, and a less sheared envelope field outside in the pre-flare magnetic configuration. Does this configuration really exist? If so, how do the sheared fields build up? How do the sheared fields evolve during the flares? Continuous observations of NOAA Active Region (AR) 10930 by Hinode (Kosugi et al. 2007) provide an opportunity for us to address these questions. AR 10930 is a complex active region, which produced four X-class flares in 2006 December; two of them were observed by both the X-ray Telescope (XRT) and the Solar Optical Telescope (SOT) aboard Hinode. In this paper, we consider the evolution of the highly sheared coronal fields prior to, during, and after the flares, in order to obtain some insights into the physics of coronal storage and release of magnetic energy.

* Movies for figure 3 are available in the electronic version ⟨http://pasj.asj.or.jp/v59/sp3/59s332/⟩.

2. Instrumentation and Data

The Hinode satellite (previously called Solar-B) is equipped with three advanced solar telescopes, i.e., XRT, SOT, and the EUV Imaging Spectrometer (EIS). It was launched on 2006 September 22 (UT). XRT is a high-resolution grazing-incidence telescope, which provides unprecedented high-resolution, high cadence observations of the X-ray corona through a wide range of filters. XRT can "see" emission for a range of temperatures, $6.1 < \log T < 7.5$, with a temperature resolution of $\Delta(\log T) = 0.2$. Temperature discrimination is achieved with a set of diagnostic filters (nine X-ray filters in total) in the focal plane. XRT also contains visible light optics. The focal-plane detector of XRT is a $2\,\mathrm{k} \times 2\,\mathrm{k}$ back-illuminated CCD with $1\farcs0$ per pixel, giving a $2000''$ field of view (FOV), which can see the entire solar disk. Details of the XRT instrumentation and the performance can be found in DeLuca et al. (2005) and Golub et al. (2007).

The G band and Ca II H data used in this study are from the Broadband Filter Imager (BFI) of SOT (Tsuneta et al. 2007). BFI produces photometric images with broad spectral resolution in 6 bands (CN band, Ca II H line, G band, and 3 continuum bands) at the highest spatial resolution available from SOT ($0\farcs0541$/pixel) and at rapid cadence (< 10 s typical) over a $218'' \times 109''$ FOV. The scientific capabilities of SOT are described in detail by Shimizu (2004). The EUV (195 Å) images used in this study were taken by TRACE, which is a high-resolution imaging telescope (Handy et al. 1999). The photospheric magnetograms were taken by SOHO/MDI. The X-ray time profiles of the two X-class flares were obtained by GOES.

Two X-class flares occurred in AR 10930 on 2006 December 13 and 14, and were observed simultaneously by XRT and SOT onboard Hinode. These two flares are the first X-class flares observed by XRT of the Hinode mission since its launch. XRT started to observe this active region at 08:52 UT on 2006 December 9, and tracked this region continuously for the remainder of its disk passage. The XRT observations of this region were obtained with the Be-thin filter from December 9 to December 14, and the temperature-response curve of this filter can be found in Golub et al. (2007). Most of the XRT images were taken with a $512'' \times 512''$ FOV and a cadence of 60 s or less. Some full FOV X-ray images were also taken occasionally as context or synoptic images. Similar to XRT, SOT was also observing this active region at the same time. The SOT G band and Ca II H images were taken with a $218'' \times 109''$ FOV and a cadence of 120 s. TRACE was observing this region at 1600 Å and white light (WL) most of the time, and some EUV (195 Å) images were also taken from time to time.

All of the XRT data used in this study were calibrated using the standard Solar Soft IDL routines. We then normalized the calibrated XRT data to its maximum value (Dmax). The logarithm of the normalized XRT data is plotted in figures 1–5 (except figure 2) and movies 1 and 2, which refer to the XRT movies of the two flares. The maximum and minimum values of the data are 0 and -1.8 for most of the XRT images and the two movies, except for figures 3b–3d, which have a minimum value of -1.2. All of the XRT images in this paper are presented in a reversed color scale, but the TRACE and SOT images are in a normal color scale. To increase the signal-to-noise ratio of some of the XRT images, we first summed a series of XRT data within 10 minutes, then divided by the number of images. This method was adopted for figures 3b, 4c, and 5c; the time presented in the corresponding figures refers to the time of the first XRT image. This technique was used only for images that are very similar to each other.

The TRACE, XRT, and SOT images are co-aligned with the MDI images by applying the following procedure. For the December 13 flare, we first determined the offset of the TRACE coordinates by aligning the TRACE WL images with the corresponding WL images taken by MDI using the location of the sunspots. We then applied this offset to the TRACE EUV images used in this study. We applied the same method to determine the offset between the SOT and MDI images. The offset between the XRT and SOT images with corrected coordinates were determined by aligning the brightenings (i.e., flare footpoints) in the SOT Ca II H line images and the corresponding XRT images. We then applied the same procedure to align the images for the December 14 flare. We applied the same offset of the XRT images obtained from the December 13 flare to the XRT images on December 10 and 12; the misalignment of the XRT, SOT, and MDI images on December 10 and 12 is estimated to be less than $3''$.

3. Results

3.1. Formation of the Sheared Magnetic Fields

The formation process of the sheared magnetic fields observed by XRT aboard Hinode and SOHO/MDI is shown in figure 1. Corresponding to the X-ray images in figures 1a and 1f, the Hinode/SOT G band images overlaid without and with MDI photospheric magnetic field contours are displayed in the top and bottom panels of figure 2. Figure 1a shows that most of the X-ray loops overlying the magnetic inversion line (MIL, marked as a thick white line) are nearly perpendicular to the MIL, which indicates that the core field was close to a potential state at 00:19 UT on 2006 December 10. The corresponding G band images in figures 2a and 2c show that AR 10930 is composed of a bipole, which contains one big sunspot with negative magnetic fields (black contours) and a small spot with positive magnetic fields (white contours). The two spots share a common penumbra. Following Moore et al. (2001), we define the core field as the fields that are rooted close to the MIL through the middle of the bipole. This core field is visible in XRT observations most of the time. Around 22:46 UT on December 10, one bright loop with an obvious higher shear shows up on the right-hand side of the core field, while there are no obvious changes in the other loops (figure 1b). About 11 hours later, two highly sheared loops were visible in the XRT obserations (figure 1c), while we still saw no shear increase in the rest of the loops. Figure 1d shows an X-ray image taken 12 hours later than that presented in figure 1c. Most of the X-ray loops in the core field region in figure 1d have a higher shear than those in figure 1c. The core field in figure 1d shows an S-shaped structure (i.e., Sigmoid) composed of two sets of disconnected loops; also, a clearer

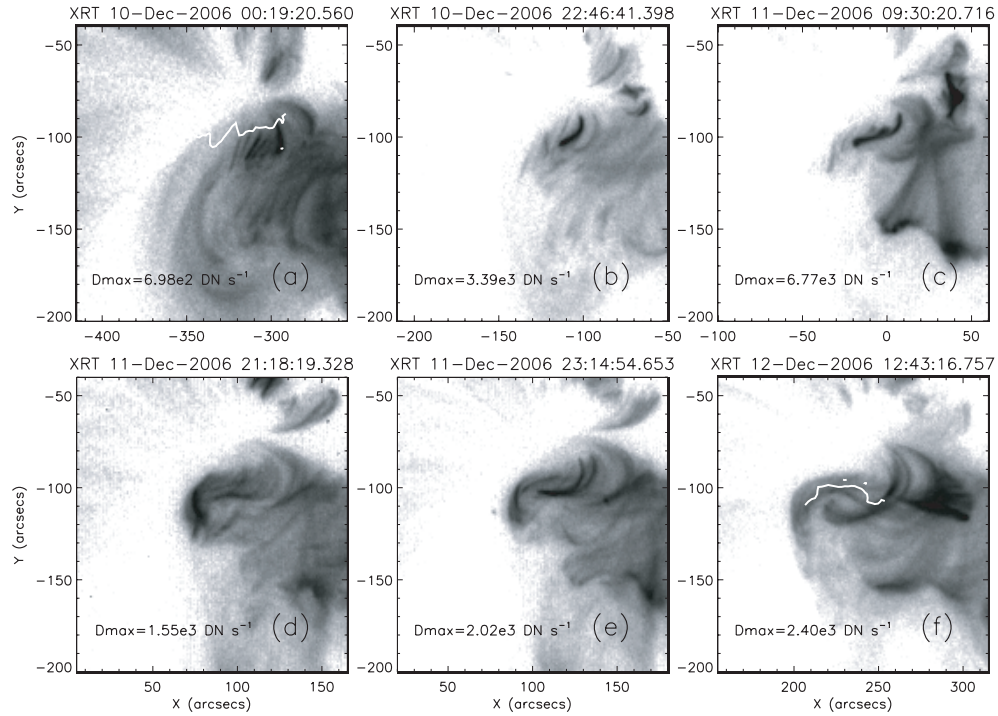

Fig. 1. Formation of the sheared magnetic fields observed by XRT aboard Hinode. (a)–(f) A series of X-ray images observed with Be-thin filter by XRT from 2006 December 10 to December 12. The maximum intensity (Dmax) of the XRT image is shown in the lower-left corner of each panel. The SOHO/MDI photospheric magnetic inversion line is represented as a thick white line.

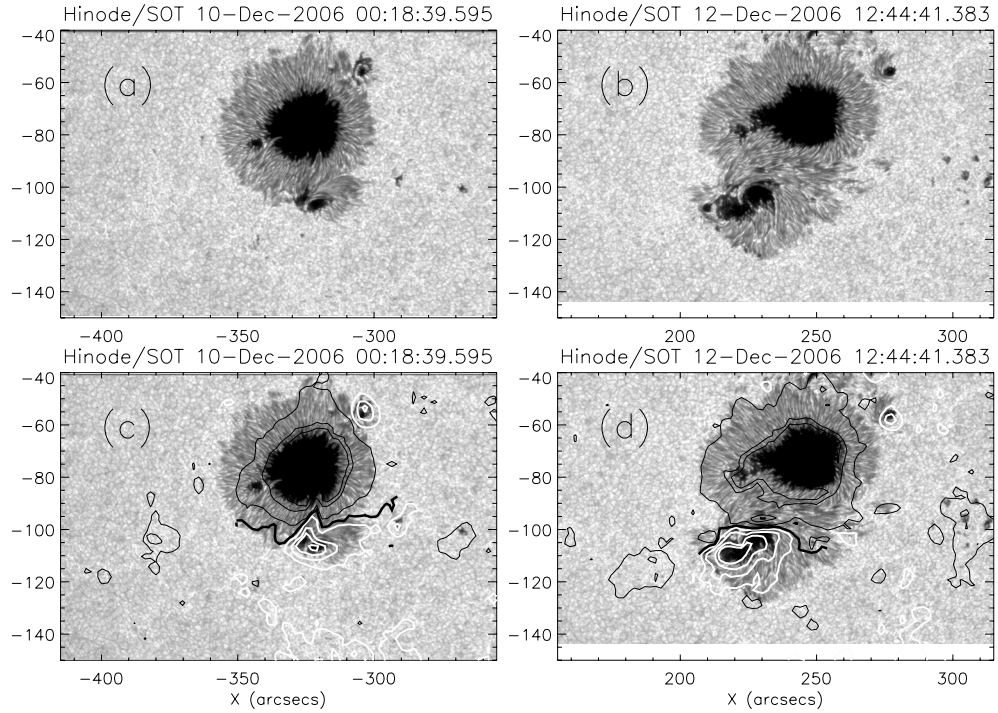

Fig. 2. Hinode/SOT G band images overlaid with SOHO/MDI magnetic contours. (a) and (b): G band images closest in time to the X-ray images in figures 1a and 1f, respectively. (c) and (d): Same G band images as in (a) and (b) overlaid with MDI magnetic contours. The white and black contours represent the positive and negative line-of-sight photospheric magnetic fields observed by MDI, and the thick black line represent the magnetic inversion line.

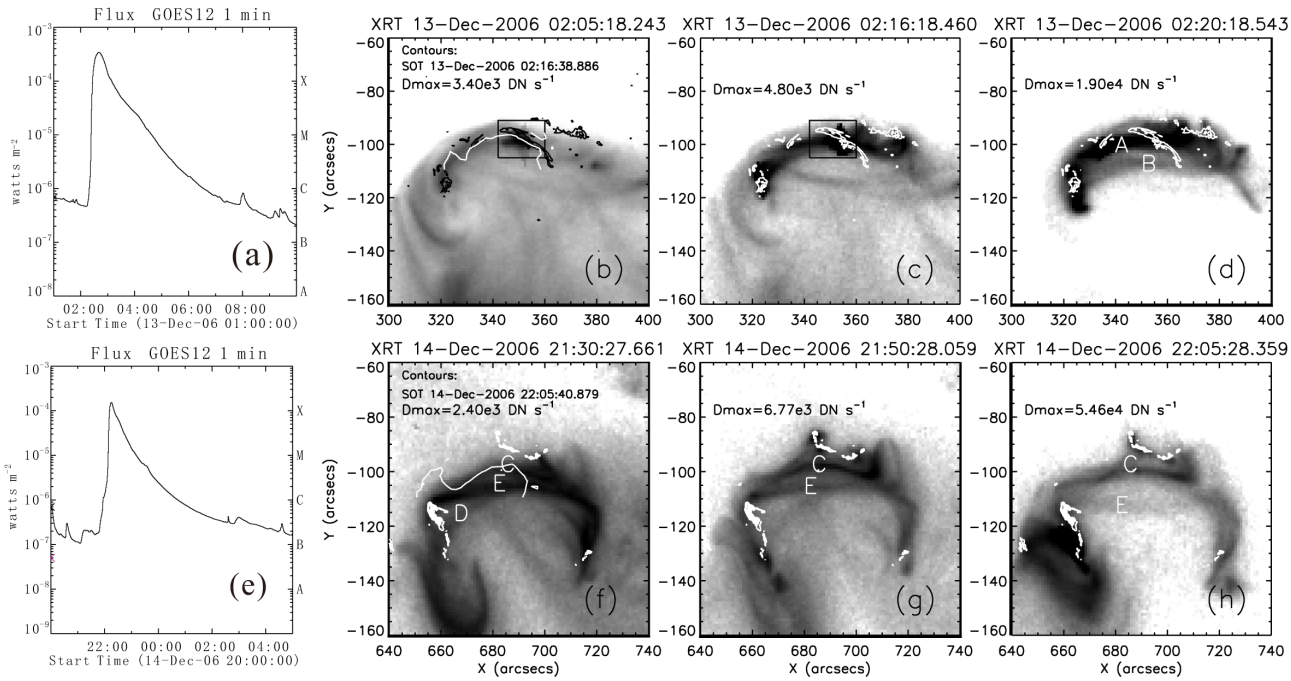

Fig. 3. XRT observations of the sheared magnetic field evolution during two X-class flares. (a) and (e): GOES X-ray time profiles for the 2006 December 13 and December 14 flares. (b) shows an XRT image prior to the December 13 flare, and two XRT images during this flare are presented in (c) and (d). The long-lasting brightening prior to the flare is enclosed by the black box in (b) and (c). The contours in (b)–(d) refer to the brightenings at 02:16 UT observed by SOT in Ca II H. (f)–(h) The XRT images at the early phase of the December 14 flare. The white contours overlaid on these images represent the brightenings at 22:05 UT on December 14 observed by SOT in Ca II H. The white lines in (b) and (f) refer to the SOHO/MDI magnetic inversion line. The maximum intensity (Dmax) of the XRT image is shown in the upper-left corner of each panel. A–E are the loops discussed in the text.

S-shaped structure can be seen in figure 1e. Most of the magnetic loops in the core field region became nearly parallel to the MIL by 12:43 UT on 2006 December 12 (figure 1f), which indicates that the coronal core field had become highly non-potential. The corresponding SOT image (figures 2b and 2d) shows that the penumbral fibrils between the two sunspots was also nearly parallel to the MIL, which indicates that the photospheric core field was also highly non-potential at this time.

Figure 1 shows that it took about two and a half days for the formation of the sheared coronal core field in AR 10930. The SOT G band and MDI movies in this time period show that the lower positive polarity spot was rotating in a counter-clockwise direction, while there is no evidence of rotation in the upper sunspot. A large amount of magnetic flux emerged to the west of the positive polarity spot, and newly emerged following flux accumulated in the spot as it rotated. A clear west-to-east motion of the lower spot can also be seen in a comparison of figures 2a and 2b. All of these observations appear to indicate that the highly sheared core field in AR 10930 is formed by this flux emergence and the accompanying rotation and west-to-east motion of the lower positive polarity sunspot.

3.2. Evolution of Sheared Magnetic Fields during the Flares

The evolution of the sheared X-ray loops observed by XRT during the December 13 and December 14 flares are presented in the top and bottom panels of figure 3, respectively. The GOES soft X-ray time profile of the December 13 flare (figure 3a) shows that it is an X3.4 flare, which started at 02:14 UT, peaked at 02:40 UT, and ended around 09:00 UT. An X-ray image prior to the flare is displayed in figure 3b, and two X-ray images from the early phase of the flare are shown in figures 3c and 3d. The black or white contours overlaid on these three X-ray images refer to the first brightenings seen in the SOT Ca II H line observations at 02:16 UT. At about 10 minutes prior to the flare, two compact brightenings in the highly sheared core field region started to appear, and the long-lasting one is shown to be enclosed by a black box in figures 3b and 3c. After the flare onset, several brightenings showed up in the footpoints of the highly sheared loops (figure 3c), and the pre-flare compact brightening still exists, which is located between the two flare footpoints. An X-ray image taken four minutes later is shown in figure 3d, which shows two highly sheared and nearly parallel loops. The fainter loop (i.e., loop B) erupted, while the brighter loop (i.e., loop A) was left behind (see movie 1*). Later on, the flare propagated to the less sheared envelope field region, which is located outside of the core field. We can see a strong-to-weak shear motion of the footpoints in the SOT Ca II H line observations during this flare, meaning that the footpoints started far apart, but close to the MIL, then moved toward each other and away from the MIL.

Figure 3e shows that the December 14 flare is an X1.5 flare, which started at 21:07 UT, peaked at 22:15 UT, and ended around 04:00 UT on December 15. Figures 3f–3h show three X-ray images at the early phase of the flare. The white contours overlaid on these three X-ray images refer to the brightenings seen in the SOT Ca II H line observations at 22:05 UT, after

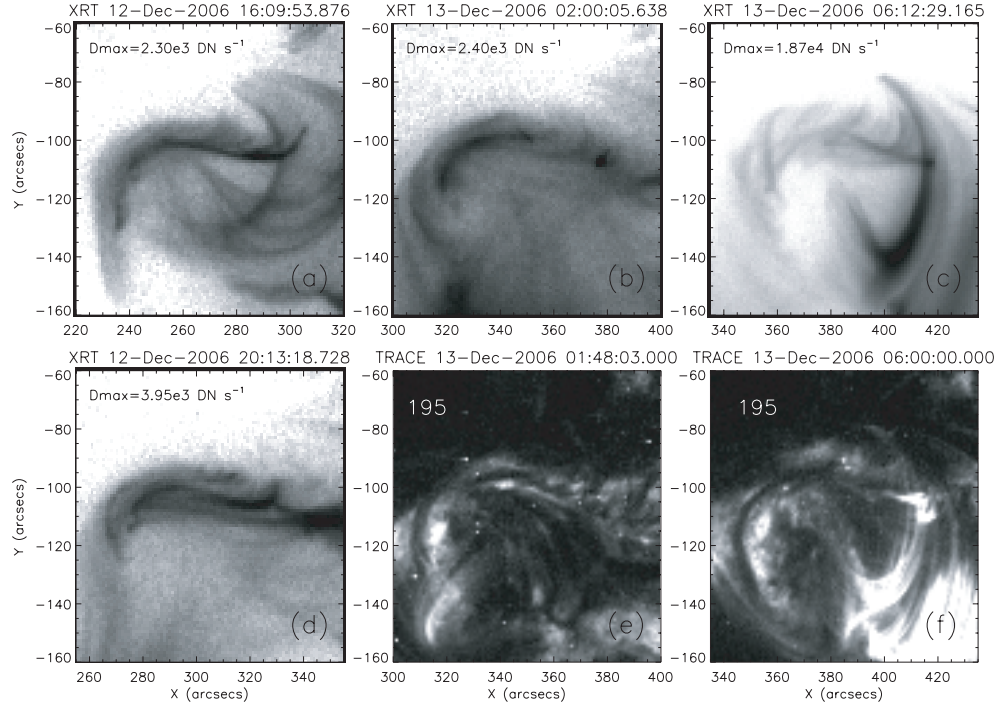

Fig. 4. Pre-flare and post-flare XRT and TRACE images of the X3.4 flare on 2006 December 13. (a), (b), and (d): Three X-ray images observed by XRT prior to the flare. (c) XRT image after the flare. (e) and (f): Two EUV images observed by TRACE prior to and after the flare for comparison with (b) and (c). The maximum intensity (Dmax) of the XRT image is shown in the upper-left corner of each panel.

which the flare ribbons started to extend along the MIL and moved away from the MIL rapidly. In the early phase, we identified three X-ray loops, i.e., loop C, loop D, and loop E, as shown in figure 3f. Loop D started to erupt around 21:26 UT (see movie 2*), after which we could see some brightenings (SOT Ca II H line) and post-flare loops (XRT) in the lower-left corner of figure 3f; some brightenings also appeared at the same position as the white contours close to loop C, which can be seen in figure 3g. From figure 3g we also see that loop E shows a continuous S-shaped structure, which is partly covered by white contours. A better view of this loop can be seen in movie 2. This S-shaped loop E started to erupt around 22:01 UT (see movie 2), which can be seen by a comparison of figures 3g and 3h. However, loop C showed no obvious motion during the entire flare process seen in the XRT observations. We also see a strong-to-weak shear motion of the footpoints in the SOT Ca II H line observations in this flare.

Both the December 13 and December 14 flares started from the highly sheared core field. In both of these flares, we can see that some of the highly sheared loops erupted, and other highly sheared loops were left behind. However, the initiation of the two flares appears to be different. In the December 13 flare, a compact brightening appeared first; we then see some brightenings (i.e., flare footpoints) located on the two opposite sides of the compact brightening. These observations indicate that magnetic reconnections may occur in the highly sheared core field, which leads to the eruption of the flare (or loop B). The loop that is left behind (i.e., loop A) appears to be a newly reconnected loop, because we see corresponding brightenings in the two ends of this loop after the flare onset. However, there is no evidence of magnetic reconnection before the eruption of loop D in the December 14 flare. After the eruption of loop D, we see some brightenings that appear to be the footpoints of the newly reconnected loops, after which loop E erupted too. The XRT movie of this flare shows that loop C that was left behind appears not to be involved in the flare process, which can also be seen in a comparison of figures 3f–3h.

3.3. Pre-Flare vs. Post-Flare Sheared Magnetic Fields

The continuous observations of AR 10930 by XRT with high spatial and temporal resolution provides us an excellent opportunity to compare the pre-flare and post-flare magnetic configurations. Figures 4a–4d show XRT observations of the core field before and after the X3.4 flare on 2006 December 13. The corresponding filaments before and after the flare observed by TRACE are displayed in figures 4e–4f. Prior to the December 13 flare, XRT had detected two loop eruptions (likely filament eruptions), which started around 16:28 and 21:58 UT on December 12, respectively. Figures 4a and 4d show the core field before and after the first loop eruption, respectively. Both of these figures show that most of the X-ray loops in the core field region were highly sheared and nearly parallel to each other, and the brightest loops had the appearance of a continuous S-shaped structure. The magnetic configuration after the second loop eruption and 14 minutes prior to the December 13 flare is displayed in figure 4b, which is composed of several highly sheared loops. After the December 13 flare onset, the post-flare loops gradually propagated from the highly sheared core field region to the outer and less-sheared envelope field region; during this time the less bright core field became invisible. Around 05:23 UT, the core field appeared again, and a clear picture

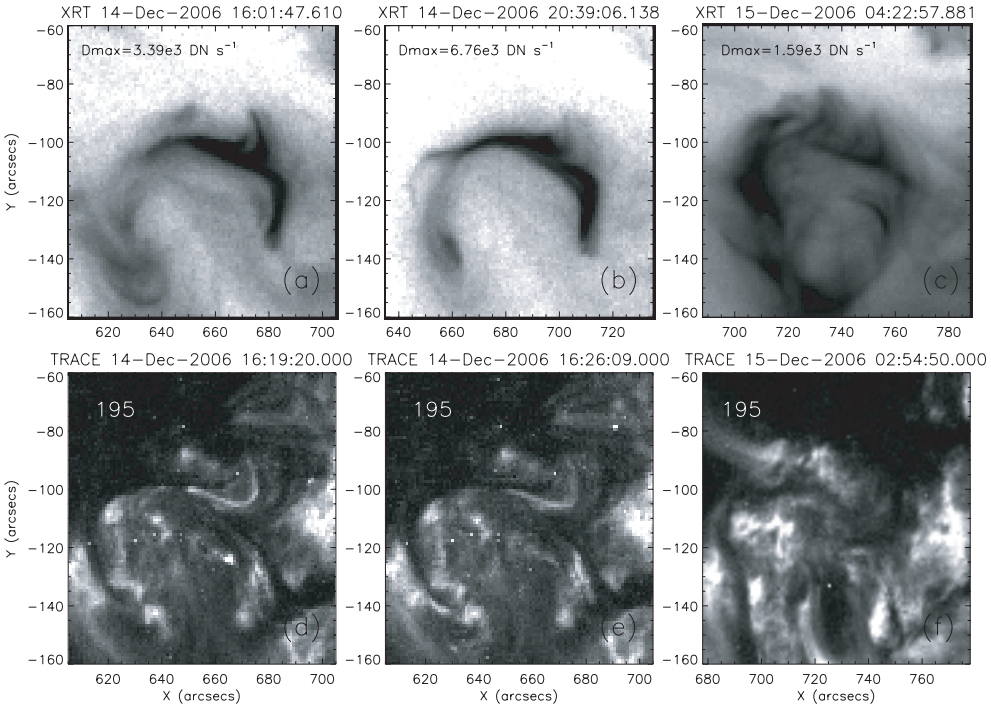

Fig. 5. Pre-flare and post-flare XRT and TRACE images for the X1.5 flare on 2006 December 14. (a) and (b): Two X-ray images observed by XRT prior to the flare. (c) XRT image after the flare. (d) and (e): Two EUV images observed by TRACE prior to the flare. (f) TRACE EUV image after the flare. The maximum intensity (Dmax) of the XRT image is shown in the upper left corner of each panel.

of the post-flare core field is displayed in figure 4c, which shows a higher sheared inner and less sheared outer structure (figure 4c). By comparing figures 4b and 4c, we can see that the post-flare core field was much less sheared than the pre-flare core field. Corresponding to the sheared core field observed by XRT, a filament is seen in TRACE prior to the December 13 flare (figure 4e). We still see most parts of the filament after the flare, as can be seen in figure 4f.

XRT images prior to and after the X1.5 flare on 2006 December 14 are shown in figures 5a–5c. The corresponding observations taken by TRACE are displayed in figures 5d–5f. A filament eruption occurred around 16:40 UT on December 14. One X-ray image prior to this eruption is shown in figure 5a, from which we see several highly sheared loops. A good TRACE image taken closest in time to figure 5a is shown in figure 5d. A comparison of the figures shows that the filament corresponds to a highly sheared X-ray loop. Figure 5b shows an X-ray image after the filament eruption and 30 minutes before the December 14 flare. We see no significant changes in the magnetic configuration before and after the filament eruption. Similar to the December 13 flare, the post-flare magnetic configuration of the December 14 flare shows a highly sheared inside and less sheared outside structure (figure 5c), and the post-flare core field is significantly less sheared than the pre-flare core field. Figure 5e shows the last good EUV image taken by TRACE prior to the December 14 flare, and a TRACE image after the flare is displayed in figure 5f. A comparison of figures 5e and 5f shows that a large part of the filament was still present after the flare.

4. Discussions and Conclusions

NOAA Active Region 10930 is a complex region, where four X-class flares occurred in 2006 December, and two of them (i.e., flares on December 13 and December 14) were observed by both XRT and SOT aboard Hinode. The continuous observations of this region by XRT and SOT provide an opportunity to study the long-term evolution of the sheared core field. In this paper, we have addressed three questions: How do non-potential magnetic fields build up? How do they evolve during flares? What is the difference between the pre-flare and post-flare magnetic configurations?

The XRT observations show that the coronal magnetic fields were close to a potential state at 00:19 UT on 2006 December 10. About 22 hours later, a shear increase started from one X-ray loop on the right-hand side of the core field rooted close to the MIL between the two main magnetic polarities. After that, more and more loops gradually became highly sheared. Most of the loops in the core field region became highly sheared and nearly parallel to the MIL around 12:43 UT on 2006 December 12. The formation of the sheared magnetic fields was caused by the counter-clockwise rotation and the west-to-east motion of the lower emerging sunspot, which can be seen in the SOT G band and Ca II H line observations as well as the SOHO/MDI observations.

Both of the X-class flares on December 13 and December 14 started from a highly sheared core field. At the early phase of each flare, some highly sheared loops erupted, and some highly sheared loops were left behind. The highly sheared loop that was left behind in the December 13 flare seems to be a newly reconnected post-flare loop. However, the one

that was left behind in the December 14 flare appears not to have been involved in any reconnection, as can be seen in the XRT observations. Corresponding to the highly sheared core field, a filament was seen in the EUV observations by TRACE prior to the two flares. A large part of the filament was still present after these two flares, which may have been caused by the fact that only part of the sheared magnetic fields erupted during the flares. The partial filament eruption is interpreted as being a partial eruption of a magnetic flux rope by Gibson and Fan (2006). The initiation of these two flares seems to be different. The X3.4 flare on December 13 appears to have been initiated by magnetic reconnection in the highly sheared core field, which agrees with the cartoon of the three-dimensional model for eruptive flares in Moore et al. (2001). However, the X1.5 flare on December 14 started from a sheared loop eruption, before which we can see no evidence of magnetic reconnection.

Two loop eruptions (likely filament eruptions) were seen by XRT prior to the December 13 flare. Most of the loops in the core field were highly sheared and nearly parallel to each other before and after the first loop eruption. The core field before both the December 13 and December 14 flares was composed of several highly sheared loops. About 2–3 hours after the peak of each flare, the core field was visible again from the XRT observations. The post-flare core field of each flare showed a higher sheared inner and less sheared outer structure, but containing significantly less shear compared to the pre-flare core field. This flare-related relaxation of magnetic shear was also found by Yohkoh/SXT (Sakurai et al. 1992). This observation is in agreement with the idea that a flare is caused by the release of magnetic energy stored in the highly sheared magnetic fields, but apparently only a fraction of the available energy is released.

A strong-to-weak shear motion of the footpoints was observed in both of two flares on December 13 and 14. This motion suggests that the pre-flare magnetic field configuration is composed of a highly sheared core field and overlying less sheared envelope field. We did not see these overlying less-sheared envelope fields in the XRT observations prior to the two flares, which is in agreement with the Yohkoh/SXT observations (Sterling et al. 2000). Moreover, a long-term XRT observation of AR 10930 shows that the core field is visible most of the time, while the overlying loops can only be seen temporarily after the flares or loop eruptions. The heating mechanism for the core field is apparently different from that of the post-flare loops. We are left with two open questions: Why do we not see the overlying unsheared sheared loops in the pre-flare phase? What is the heating mechanism of the core field?

We thank the anonymous referee and the editors for valuable suggestions to improve this paper. Hinode is a Japanese mission developed and launched by ISAS/JAXA, with NAOJ as domestic partner and NASA and STFC (UK) as international partners. It is operated by these agencies in co-operation with ESA and the NSC (Norway). US members of the XRT team are supported by NASA contract NNM07AA02C to Smithsonian Astrophysical Observatory (SAO). The TRACE analyses are supported at SAO by a contract from Lockheed Martin. Y. Su is also supported by an SAO pre-doctoral Fellowship, the NSFC projects with 10333030 and 10273025, and "973" program with 2006CB806302.

References

Canfield, R. C., Hudson, H. S., & McKenzie, D. E. 1999, Geophys. Res. Lett., 26, 627

DeLuca, E. E., Weber, M. A., Sette, A. L., Golub, L., Shibasaki, K., Sakao, T., & Kano, R. 2005, Adv. Space Res., 36, 1489

Gibson, S. E., & Fan, Y. 2006, ApJ, 637, L65

Golub, L., et al. 2007, Sol. Phys., 243, 63

Handy, B. N., et al. 1999, Sol. Phys., 187, 229

Ji, H., Huang, G., & Wang, H. 2007, ApJ, 660, 893

Ji, H., Huang, G., Wang, H., Zhou, T., Li, Y., Zhang, Y., & Song, M. 2006, ApJ, 636, L173

Kosugi, T., et al. 2007, Sol. Phys., 243, 3

Masuda, S., Kosugi, T., & Hudson, H. S. 2001, Sol. Phys., 204, 55

Moore, R. L., Sterling, A. C., Hudson, H. S., & Lemen, J. R. 2001, ApJ, 552, 833

Priest, E. R., & Forbes, T. G. 2002, A&AR, 10, 313

Rust, D. M., & Kumar, A. 1996, ApJ, 464, L199

Sakurai, T., Shibata, K., Ichimoto, K., Tsuneta, S., & Acton, L. W. 1992, PASJ, 44, L123

Shimizu, T. 2004, in ASP Conf. Ser. 325, The Solar-B Mission and the Forefront of Solar Physics, ed. T. Sakurai & T. Sekii (San Francisco: ASP), 3

Sterling, A. C., Hudson, H. S., Thompson, B. J., & Zarro, D. M. 2000, ApJ, 532, 628

Su, Y., Golub, L., & van Ballegooijen, A. A. 2007a, ApJ, 655, 606

Su, Y., Golub, L., van Ballegooijen, A. A., & Gros, M. 2006, Sol. Phys., 236, 325

Su, Y., van Ballegooijen, A., McCaughey, J., DeLuca, E., Reeves, K. K., & Golub, L. 2007b, ApJ, 665, 1448

Tsuneta, S., et al. 2007, Sol. Phys. submitted